

Characteristic local association of In impurities dispersed in ZnO

W. Sato,^{1,2} S. Komatsuda,² and Y. Ohkubo³

¹*Institute of Science and Engineering, Kanazawa University, Kanazawa, Ishikawa 920-1192, Japan*

²*Graduate School of Natural Science and Technology, Kanazawa University, Kanazawa, Ishikawa 920-1192, Japan*

³*Research Reactor Institute, Kyoto University, Kumatori, Osaka 590-0494, Japan*

(Received 3 August 2012; published 28 December 2012)

Local environments in 0.5 at.% In-doped ZnO were investigated by means of the time-differential perturbed angular correlation (TDPAC) method. In a comparative study, using the ^{111}Cd probe nuclei as the decay products of different parents, ^{111}In and $^{111\text{m}}\text{Cd}$, we found that ^{111}In microscopically forms a unique structure with nonradioactive In ion(s) dispersed in ZnO, whereas $^{111\text{m}}\text{Cd}$ has no specific interaction with the In impurities. The spectral damping of the TDPAC spectra is attributed to the aftereffect following the EC decay of ^{111}In . It was demonstrated from the aftereffect that the local density and/or mobility of conduction electrons at the ^{111}In probe site in the In-doped ZnO is lowered due to the characteristic structure locally formed by the dispersed In ion(s).

DOI: [10.1103/PhysRevB.86.235209](https://doi.org/10.1103/PhysRevB.86.235209)

PACS number(s): 76.80.+y, 61.72.uj, 72.80.Ey

I. INTRODUCTION

Zinc oxide (ZnO) is an intrinsic *n*-type II-VI compound semiconductor having a wide band gap of 3.4 eV, and its optically transparent conductivity is very desirable for applications in various fields of technology. Apart from the intrinsic property brought about by defects created in its synthesis process, the electric conductivity of ZnO is variable depending on how, how many, and what kind(s) of impurities are doped in the matrix.^{1–4} It has also been known by recent studies that codoping of impurities of different elements exhibits intriguing properties leading to future spintronic devices.^{5–7} In order to understand such impurity-induced physical properties, it is of great importance to investigate the interacting nature of impurities in ZnO by obtaining atomic-level information on their ambient electric and/or magnetic fields.^{8–14}

For investigation of the electromagnetic fields in the vicinity of dilute impurities incorporated in ZnO, we applied the time-differential perturbed angular correlation (TDPAC) method to our recent studies on ZnO.^{15–17} The TDPAC method is a nuclear spectroscopic technique, which provides local information in matter through electromagnetic interactions between probe nuclei and the surrounding spins and charge distribution.^{18,19} In a series of our TDPAC studies, we employed the ^{111}Cd probe formed in the process of the electron capture (EC) decay of ^{111}In . This probe satisfies the present purpose because the parent nuclide, ^{111}In , is generally considered to be an ideal donor in the system of this II-VI compound and, hence, can provide direct information on the local structure at the donor site. Applying this spectroscopy, we obtained the following results for 0.5 at.% In-doped ZnO:¹⁵ (i) a single high-frequency component predominates in the TDPAC spectra, showing that the electric field gradient (EFG) at the probe is distinctly larger than the one observed for undoped ZnO, and (ii) the spectral damping, which is observed for undoped ZnO as well, is obviously enhanced for the In-doped, especially at lower temperature. Because these observations for the 0.5 at.% In-doped ZnO are significantly different from those for the undoped, it is undoubted that the doped In impurities form a unique structure to give rise to the high quadrupole frequency and the marked spectral damping. As for the damping trend, we suggested that the phenomenon

could be caused by a so-called aftereffect accompanying the EC decay.¹⁵ However, there remains a question why this phenomenon is more pronounced in the In-doped ZnO than the undoped in spite of the presence of In ions in the system. Do the dilute In ions truly function as a donor in ZnO as is commonly expected? In order to answer this question, it is important to clarify if this strong damping observed for the 0.5 at.% In-doped ZnO is characteristic of the $^{111}\text{Cd}(\leftarrow^{111}\text{In})$ probe or it goes for other probes as well. We have thus performed TDPAC measurements introducing in In-doped ZnO the same probe but descended from a different parent nucleus via an isomeric transition (IT), $^{111}\text{Cd}(\leftarrow^{111\text{m}}\text{Cd})$. In the present paper, distinct interacting natures between nonradioactive In impurities and the probes (^{111}Cd) formed in the disintegration of different parents (^{111}In and $^{111\text{m}}\text{Cd}$) are discussed based on the EFGs at the probes and on their spectral amplitudes.

II. EXPERIMENT

We initially examined the site occupied by the $^{111}\text{Cd}(\leftarrow^{111\text{m}}\text{Cd})$ probe in ZnO lattice according to the following procedure. About 3 mg of cadmium oxide (CdO) enriched with ^{110}Cd was irradiated with thermal neutrons in a pneumatic tube at Kyoto University Reactor, and radioactive $^{111\text{m}}\text{Cd}$ was generated by the $^{110}\text{Cd}(n, \gamma)^{111\text{m}}\text{Cd}$ reaction. The neutron-irradiated CdO powder was then added into stoichiometric amount of ZnO powder to synthesize 0.5 at.% Cd-doped ZnO. The powders were thoroughly mixed in a mortar. The mixture was then pressed into a disk, and sintered in air at 1373 K for 45 min. A TDPAC measurement was carried out for the $^{111}\text{Cd}(\leftarrow^{111\text{m}}\text{Cd})$ probe on the 151–245 keV cascade γ rays with the intermediate state of $I^\pi = 5/2^+$ having a half-life of 85.0 ns.²⁰ A simplified decay scheme of $^{111}\text{Cd}(\leftarrow^{111\text{m}}\text{Cd})$ is shown in Fig. 1 along with the one of $^{111}\text{Cd}(\leftarrow^{111}\text{In})$. For the γ -ray detection, BaF₂ scintillation detectors were adopted due to their excellent time resolution.

After ascertaining the residence site of the $^{111}\text{Cd}(\leftarrow^{111\text{m}}\text{Cd})$ probe, which is described in Sec. III A, we investigated the interacting nature of In and Cd ions in the following manner. Stoichiometric amount of $\text{In}(\text{NO}_3)_3 \cdot 3\text{H}_2\text{O}$ of a purity of 99.99% was dissolved in ethanol, and then ZnO powder (99.999%) was added in the solution to produce 0.5 and 2 at.%

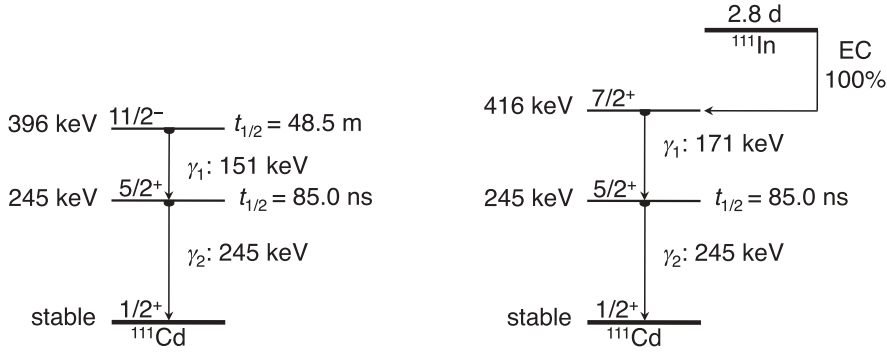


FIG. 1. Simplified decay schemes of the ^{111}Cd probe descended from different parents, $^{111\text{m}}\text{Cd}$ and ^{111}In .

In-doped ZnO. Each suspension was heated to dryness while stirred on a magnetic stirrer. The uniformly mixed powders were then pressed into disks, and they were sintered on a platinum plate in air at 1273 K for 3 h. Cadmium oxide powder including the $^{111}\text{Cd}(\leftarrow^{111\text{m}}\text{Cd})$ probe prepared in the same way as above was mixed with the In-doped ZnO samples. The mixtures were subsequently pressed into disks and sintered in air at 1373 K for 45 min. TDPAC measurements were performed for the samples at room temperature.

In order to scrutinize the damping nature of a spectrum of the $^{111}\text{Cd}(\leftarrow^{111}\text{In})$ probe in undoped ZnO, an undoped sample was prepared by the following procedure. Droplets of ^{111}In HCl solution were added onto a disk of undoped ZnO sintered in advance in air at 1273 K, and it was then heated in air at 1373 K for 2 h for diffusion of the probe. In the TDPAC measurement, a large number of coincidence events were accumulated for better counting statistics than before.¹⁵

In the present work, we obtained the directional anisotropy as a function of the time interval of the cascade γ -ray emissions by the following arithmetic operation:

$$A_{22}G_{22}(t) = \frac{2[N(\pi, t) - N(\pi/2, t)]}{N(\pi, t) + 2N(\pi/2, t)}, \quad (1)$$

where A_{22} denotes the angular correlation coefficient representing the magnitude of the directional anisotropy of the cascade γ rays, $G_{22}(t)$ the time-differential perturbation factor as a function of the time interval, t , between the cascade γ -ray emissions, and $N(\theta, t)$ the number of the delayed coincidence events observed at an angle, θ .

In this paper, abbreviations are used for simplicity to denominate ZnO samples doped with different nonradioactive impurity atoms and TDPAC probes as listed in Table I.

III. RESULTS AND DISCUSSION

A. Residence site of the $^{111}\text{Cd}(\leftarrow^{111\text{m}}\text{Cd})$ probe

The TDPAC spectra for $^{111\text{m}}\text{Cd}$ -CZO and $^{111\text{m}}\text{Cd}$ -ICZO are shown in Fig. 2. It is to be noted that the 0.5 at.% nonradioactive

Cd is inevitably incorporated in the sample because the nuclear isomer $^{111\text{m}}\text{Cd}$ cannot be chemically separated from the stable ^{110}Cd in the irradiated CdO. The oscillatory structure observed in Fig. 2(a) is typical of the perturbation pattern reflecting an axially symmetric static electric quadrupole interaction for the nuclear spin $I = 5/2$. Assuming a symmetric static EFG, we carried out a least-squares fit to the spectrum in Fig. 2(a) using the following time-differential perturbation factor, $G_{22}^{\text{static}}(t)$:

$$G_{22}^{\text{static}}(t) = \frac{1}{5} \left[1 + \frac{13}{7} \cos(6\omega_Q t) + \frac{10}{7} \cos(12\omega_Q t) + \frac{5}{7} \cos(18\omega_Q t) \right], \quad (2)$$

where ω_Q stands for the nuclear quadrupole frequency proportional to one of the principal components of the EFG tensor, V_{zz} , and t is the time interval between the cascade γ -ray emissions. The EFG value obtained for the spectrum in Fig. 2(a) is $1.7(3) \times 10^{21} \text{ Vm}^{-2}$, showing a good agreement with theoretical values deduced for a Cd^{2+} ion residing at the Zn site (1.565×10^{21} and $1.68 \times 10^{21} \text{ Vm}^{-2}$).^{21,22} It was found from this observation that the $^{111}\text{Cd}(\leftarrow^{111\text{m}}\text{Cd})$ probe, in the same way as the case for $^{111}\text{Cd}(\leftarrow^{111}\text{In})$,^{8,11–13,15,22,23} occupies the substitutional Zn site in spite of as large a difference as 30% in the ionic radius between Cd^{2+} (78 pm) and Zn^{2+} (60 pm) with the coordination number of 4 and does not feel the field produced by other nonradioactive Cd ions; that is, Cd ions are widely dispersed in the ZnO matrix so that there is little, if any, mutual interaction between themselves.

B. Interactions of the probes with nonradioactive In impurities

Figures 2(b) and 2(c) show the TDPAC spectra for $^{111\text{m}}\text{Cd}$ -ICZO doped (b) with 0.5 at.% and (c) with 2 at.% In measured at room temperature. The spectral patterns for both $^{111\text{m}}\text{Cd}$ -ICZO are analogous to the one for $^{111\text{m}}\text{Cd}$ -CZO in Fig. 2(a); least-squares fits were thus performed with the perturbation function in Eq. (2).²⁴ We have obtained the following two

TABLE I. Abbreviations for ZnO samples doped with impurity atoms and TDPAC probes.

Abbreviations	Nonradioactive Impurity Atoms (Concentrations)	PAC Probes (\leftarrow Parents)
^{111}In -UZO	None	$^{111}\text{Cd}(\leftarrow^{111}\text{In})$
^{111}In -IZO	In(0.5 at.%)	$^{111}\text{Cd}(\leftarrow^{111}\text{In})$
$^{111\text{m}}\text{Cd}$ -CZO	Cd(0.5 at.%)	$^{111}\text{Cd}(\leftarrow^{111\text{m}}\text{Cd})$
$^{111\text{m}}\text{Cd}$ -ICZO	In(0.5 or 2 at.%) and Cd(0.5 at.%)	$^{111}\text{Cd}(\leftarrow^{111\text{m}}\text{Cd})$

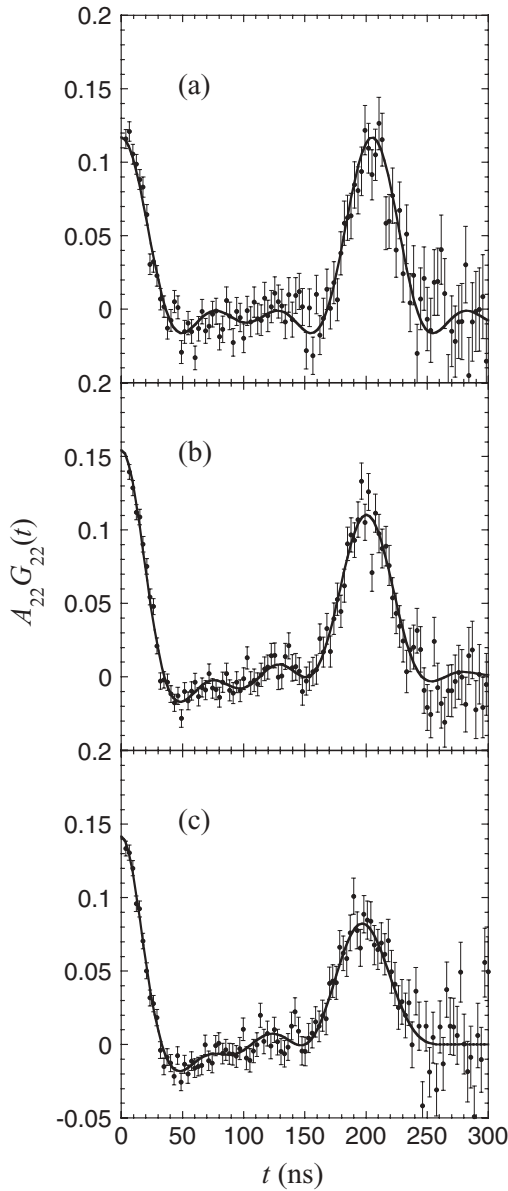


FIG. 2. TDPAC spectra of $^{111}\text{Cd}(\leftarrow^{111\text{m}}\text{Cd})$ (a) in 0.5 at.% Cd-doped ZnO, (b) in 0.5 at.% Cd- and 0.5 at.% In-doped ZnO, and (c) in 0.5 at.% Cd- and 2 at.% In-doped ZnO measured at room temperature. Least-squares fits were performed with Eq. (2) for the perturbation factors. For the spectra in (b) and (c), the normal distribution is assumed for the quadrupole frequency.

results from the fits: (1) the magnitude of the EFG at the probe was estimated to be $1.8(3) \times 10^{21} \text{ Vm}^{-2}$ for both, which agrees well with that for $^{111\text{m}}\text{Cd}$ -CZO, and (2) in comparison with $^{111\text{m}}\text{Cd}$ -CZO, the distribution of the quadrupole frequencies becomes greater with increasing concentration of the doped In. [$\delta = 4.0$ (15)% and 6.4 (15)% for the spectra (b) and (c), respectively, where δ represents the relative width to the centroid of the nuclear quadrupole frequency.]

The observation (1) demonstrates that the ^{111}Cd probe doped in $^{111\text{m}}\text{Cd}$ -ICZO resides at the substitutional Zn site regardless of the presence of In impurities in the system. The oscillatory structure of the spectra is thus completely different from that for the case of the $^{111}\text{Cd}(\leftarrow^{111}\text{In})$ probe in 0.5 at.%

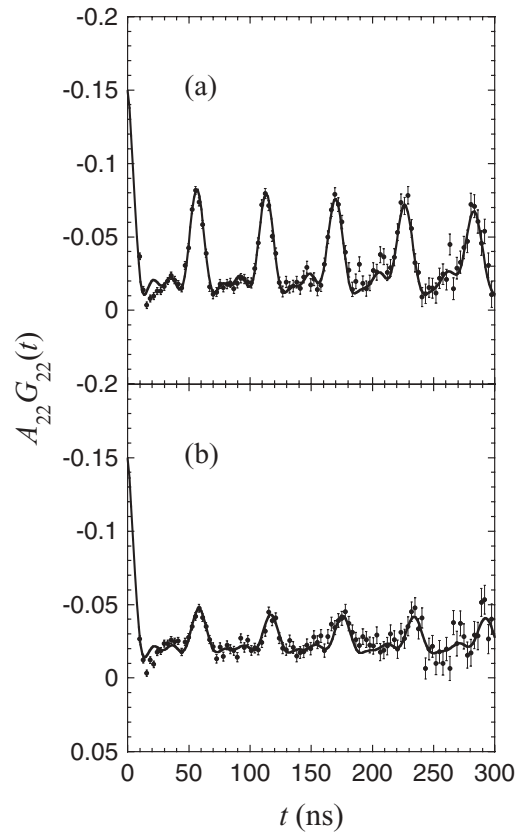


FIG. 3. TDPAC spectra of $^{111}\text{Cd}(\leftarrow^{111}\text{In})$ in 0.5 at.% In-doped ZnO measured (a) at 1000 K and (b) at room temperature. Least-squares fits were performed with Eq. (3) for the perturbation factors.

In-doped ZnO (^{111}In -IZO) as cited in Fig. 3,¹⁵ which exhibits an explicit perturbation pattern with a single high-frequency component. These distinct observations obtained with the same ^{111}Cd probes formed in the disintegration of the different parents ($^{111\text{m}}\text{Cd}$ and ^{111}In) lead to the consequence: it is the ^{111}Cd probe as the EC decay product of ^{111}In but not as the IT product of $^{111\text{m}}\text{Cd}$ that has a characteristic interaction with the coexisting nonradioactive In ion(s). Accordingly, it was found that the nonradioactive In ion(s) are adjacent to $^{111}\text{Cd}(\leftarrow^{111}\text{In})$ to produce a unique field at the probe.

The above discussion on the In site leads one to an interpretation that In ions associate with each other; however, it is still unknown how the association resides in ZnO matrix. The distribution of the quadrupole frequency can be an index of diversity of the environment surrounding the $^{111}\text{Cd}(\leftarrow^{111\text{m}}\text{Cd})$ probe. In view of this, the above observation (2) provides a finding that each In site is randomly dispersed. We hence propose from all the experimental evidences that In ions are locally associated with each other, on a microscopic scale beyond the resolving power of X-ray diffraction,^{15,25} and each small unit of the association is independently scattered in the sample forming a fixed local structure. It is to be noted, however, that the possibility of the formation of indium oxide phases can be ruled out since the present spectral pattern is obviously different from the reported one for In_2O_3 .²⁶

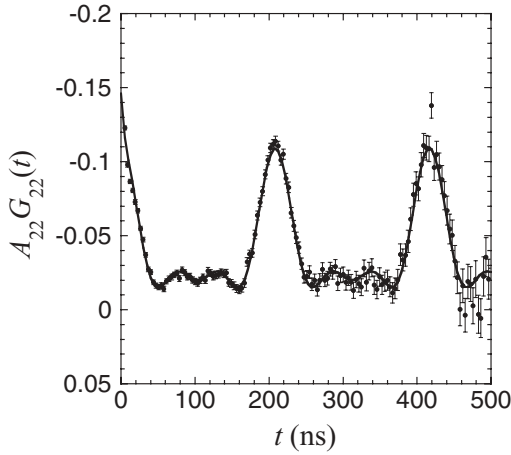


FIG. 4. TDPAC spectrum of $^{111}\text{Cd}(\leftarrow^{111}\text{In})$ in undoped ZnO measured at room temperature. A least-squares fit was performed with Eq. (3) for the perturbation factor.

C. Spectral damping by the aftereffect following the EC decay

The oscillatory structure in the TDPAC spectrum for ^{111}mCd -CZO in Fig. 2(a) keeps its amplitude constant at the initial value at $t = 0$ ns for at least the present time window of observation, whereas the oscillation peaks in the spectrum for ^{111}In -UZO in Fig. 4 are equally damped compared with the initial value. Considering that both ^{111}Cd probes occupy the substitutional Zn site, these contrastive results should be ascribed to the difference in their parents, ^{111}In and ^{111}mCd . Assuming the aftereffect, therefore, the spectrum for ^{111}In -UZO in Fig. 4, as well as those for ^{111}In -IZO in Fig. 3, was analyzed using the following perturbation factor, $G_{22}(t)$, developed by B  verstam *et al.*:²⁷

$$G_{22}(t) = G_{22}^*(t)G_{22}^{\text{static}}(t). \quad (3)$$

Here, $G_{22}^*(t)$ is the time-dependent dynamic perturbation part for the damping effect on the static perturbation, $G_{22}^{\text{static}}(t)$. The $G_{22}^*(t)$ is expressed as

$$G_{22}^*(t) = \frac{\lambda_g}{\lambda_g + \lambda_r} + \frac{\lambda_r}{\lambda_g + \lambda_r} \exp[-(\lambda_g + \lambda_r)t], \quad (4)$$

where λ_g is defined as the reciprocal of the recovery time, τ_g , to the ground state of the probe atom, and λ_r stands for the Abragam and Pound relaxation constant.²⁸ The perturbation pattern is reproduced well by the fit. This analytical method was also adopted for ^{111}In in undoped ZnO by Mu  oz *et al.*²² They examined the aftereffect in a wide temperature range, showing temperature variation of the above hyperfine parameters. In addition, their *ab initio* calculations successfully revealed the defect-free substitution of Cd^{2+} at the lattice Zn site, and discussion was extended to the correlation between the parameters and electronic state of the Cd ion. We are thus convinced from all the experimental evidences that the damped structure seen in the spectrum for ^{111}In -UZO has been induced by the aftereffect characteristic of the EC decay of ^{111}In .

In general, the EC decay is followed by the rearrangement of electrons in the atomic orbital in which the positive holes created by the radioactive decay process are refilled with conduction electrons. The charge distribution surrounding the

probe nucleus drastically changes during the corresponding time of the refilling process, resulting in the time-dependent EFG at the probe. The aftereffect is the phenomenon that the angular correlation of the cascade γ rays is averaged as a result of the dynamic perturbation by the time-variant EFG; the relevant effect thus becomes pronounced when the refilling process is slow, in other words, when the dynamic perturbation lasts long. Because the concentration of conduction electrons generally increases in semiconductors as the temperature is raised, the refilling process ends up more rapidly than at low temperature. The temperature dependence of the spectral amplitude seen in Fig. 3 is an evident proof of the difference in the local availability of conduction electrons at the probe ions in ZnO as a semiconductor.

In addition to the temperature dependence, it is obvious that the damping trend is enhanced for the spectra of ^{111}In -IZO in Fig. 3, especially for the room-temperature spectrum in Fig. 3(b), compared with the case for ^{111}In -UZO shown in Fig. 4. Our analysis shows that the λ_g values are smaller at any observed temperature for ^{111}In -IZO than those for ^{111}In -UZO.¹⁵ This result signifies that the refilling process after the EC decay takes a longer time for ^{111}In -IZO than for the undoped because of less availability of outer surrounding electrons. This phenomenon should be attributed to the environmental difference surrounding the $^{111}\text{Cd}(\leftarrow^{111}\text{In})$ probe, which directly interacts with the macroscopically doped nonradioactive In ion(s). If the doped In^{3+} ions provide additional conduction electrons to the system and the electrons can move around at least to the same degree as in undoped ZnO, the aftereffect should be suppressed in the In-doped ZnO. The present observations evidently show that the unique local structure created by the In ion(s) lowers the local density and/or mobility of conduction electrons at the $^{111}\text{Cd}(\leftarrow^{111}\text{In})$ probe by some mechanism such as electron scattering.

IV. SUMMARY AND CONCLUSIONS

The local structure and availability of conduction electrons at an impurity, In, doped in ZnO were investigated by means of the TDPAC method by a comparative study using identical probes but descended from different parents, $^{111}\text{Cd}(\leftarrow^{111}\text{In})$ and $^{111}\text{Cd}(\leftarrow^{111}\text{mCd})$. The magnitude of the EFG at the $^{111}\text{Cd}(\leftarrow^{111}\text{mCd})$ probe site observed for ^{111}mCd -CZO agrees well with the corresponding value for ^{111}In -UZO, suggesting that ^{111}mCd substitutes for Zn site in spite of the large ionic radius. For ^{111}mCd -ICZO samples, it was found that the $^{111}\text{Cd}(\leftarrow^{111}\text{mCd})$ probe also resides at substitutional Zn site with no specific interaction with neither Cd nor In impurity ions. This observation reveals that it is only the $^{111}\text{Cd}(\leftarrow^{111}\text{In})$ probe that has a characteristic interaction with nonradioactive In impurities in ZnO. The increasing distribution of the EFG at the $^{111}\text{Cd}(\leftarrow^{111}\text{mCd})$ probe along with the concentration of In ions is a proof that the doped In ions are widely dispersed in the sample without forming macroscopic phase(s) of In aggregations. For ^{111}mCd -CZO, notable damping of spectral amplitude as seen for ^{111}In -UZO was not observed, which signifies that the damped structure in ^{111}In -UZO is ascribable to the aftereffect of the EC decay. The unequivocal damping of the oscillatory structure in the spectrum for ^{111}In -IZO especially at room temperature suggests that the

local density and/or mobility of conduction electrons at the $^{111}\text{Cd}(\leftarrow^{111}\text{In})$ probe adjacent to In ion(s) in 0.5 at.% In-doped ZnO is lowered by the characteristic local structure formed by the In ion(s).

The microscopic In complex is expected to be a key to the development of new semiconductor devices. Detailed structural information is now under investigation.

ACKNOWLEDGMENTS

We express our gratitude to Y. Yamada for helpful discussion on the probe site. We also thank T. Saito and Y. Yamaguchi of Osaka University for providing experimental apparatus. The present work was accomplished as part of the Visiting Researcher's Program of the Kyoto University Research Reactor Institute (KURRI).

- ¹V. Bhosle, A. Tiwari, and J. Narayan, *J. Appl. Phys.* **100**, 033713 (2006).
- ²J. Han, P. Q. Mantas, and A. M. R. Senos, *J. Eur. Ceram. Soc.* **21**, 1883 (2001).
- ³B. D. Ahn, S. H. Oh, H. J. Kim, M. H. Jung, and Y. G. Ko, *Appl. Phys. Lett.* **91**, 252109 (2007).
- ⁴B. K. Meyer, H. Alves, D. M. Hofmann, W. Kriegseis, D. Forster, F. Bertram, J. Christen, A. Hoffmann, M. Straßburg, M. Dworzak, U. Haboeck, and A. V. Rodina, *Phys. Status Solidi B* **241**, 231 (2004).
- ⁵A. J. Behan, A. Mokhtari, H. J. Blythe, D. Score, X-H. Xu, J. R. Neal, A. M. Fox, and G. A. Gehring, *Phys. Rev. Lett.* **100**, 047206 (2008).
- ⁶Y. He, P. Sharma, K. Biswas, E. Z. Liu, N. Ohtsu, A. Inoue, Y. Inada, M. Nomura, J. S. Tse, S. Yin, and J. Z. Jiang, *Phys. Rev. B* **78**, 155202 (2008).
- ⁷A. Ney, V. Ney, S. Ye, K. Ollefs, T. Kammermeier, T. C. Kaspar, S. A. Chambers, F. Wilhelm, and A. Rogalev, *Phys. Rev. B* **82**, 041202(R) (2010).
- ⁸S. Müller, D. Stichtenoth, M. Uhrmacher, H. Hofsäss, C. Ronning, and J. Röder, *Appl. Phys. Lett.* **90**, 012107 (2007).
- ⁹H. P. Gunnlaugsson, T. E. Møhlholt, R. Mantovan, H. Masenda, D. Naidoo, W. B. Dlamini, R. Sielemann, K. Bharuth-Ram, G. Weyer, K. Johnston, G. Langouche, S. Ólafsson, H. P. Gíslason, Y. Kobayashi, Y. Yoshida, and M. Fanciulli, *Appl. Phys. Lett.* **97**, 142501 (2010).
- ¹⁰G. Weyer, H. P. Gunnlaugsson, R. Mantovan, M. Fanciulli, D. Naidoo, K. Bharuth-Ram, and T. Agne, *J. Appl. Phys.* **102**, 113915 (2007).
- ¹¹Th. Agne, Z. Guan, X. M. Li, H. Wolf, Th. Wichert, H. Natter, and R. Hempelmann, *Appl. Phys. Lett.* **83**, 1204 (2003).
- ¹²E. Rita, J. G. Correia, U. Wahl, E. Alves, A. M. L. Lopes, J. C. Soares, and The ISOLDE Collaboration, *Hyperfine Interact.* **158**, 395 (2004).
- ¹³R. Dogra, A. P. Byrne, and M. C. Ridgway, *J. Electron. Mater.* **38**, 623 (2009).
- ¹⁴A. F. Pasquevich and M. Renteria, *Defect Diffus. Forum* **311**, 62 (2011).
- ¹⁵W. Sato, Y. Itsuki, S. Morimoto, H. Susuki, S. Nasu, A. Shinohara, and Y. Ohkubo, *Phys. Rev. B* **78**, 045319 (2008).
- ¹⁶W. Sato, Y. Komeno, M. Tanigaki, A. Taniguchi, S. Kawata, and Y. Ohkubo, *J. Phys. Soc. Jpn.* **77**, 105001 (2008).
- ¹⁷S. Komatsuda, W. Sato, S. Kawata, and Y. Ohkubo, *J. Phys. Soc. Jpn.* **80**, 095001 (2011).
- ¹⁸H. Frauenfelder and R. M. Steffen, in *α -, β -, and γ -Ray Spectroscopy*, edited by K. Siegbahn (North-Holland, Amsterdam, 1965), Vol. 2, p. 997.
- ¹⁹G. Schatz and A. Weidinger, *Nuclear Condensed Matter Physics* (Wiley, New York, 1996).
- ²⁰R. B. Firestone, in *Table of Isotopes*, edited by V. S. Shirley, 8th ed. (Wiley, New York, 1996), Vol. 1.
- ²¹Y. Abreu, C. M. Cruz, P. V. Espen, C. Pérez, I. Piñera, A. Leyva, and A. E. Cabal, *Solid State Commun.* **152**, 399 (2012).
- ²²E. L. Muñoz, M. E. Mercurio, M. R. Cordeiro, L. F. D. Pereira, A. W. Carbonari, and M. Renteira, *Physica B* **407**, 3121 (2012).
- ²³H. Wolf, S. Deubler, D. Forkel, H. Foettinger, M. Iwatschenko-Borho, F. Meyer, M. Renn, W. Witthuhn, and R. Helbig, *Mater. Sci. Forum* **10–12**, 863 (1986).
- ²⁴One can see a little undulation at around 130 ns, which might have arisen from the insufficient heat treatment during the sample preparation due to the short half-life of $^{111\text{m}}\text{Cd}$. In the present analysis, this unknown structure was reproduced assuming the presence of another minor component.
- ²⁵W. Sato, Y. Ohkubo, Y. Itsuki, S. Komatsuda, D. Minami, T. Kubota, S. Kawata, A. Yokoyama, and T. Nakanishi, *Proc. Radiochim. Acta* **1**, 435 (2011).
- ²⁶A. G. Bibiloni, J. Desimoni, C. P. Massolo, L. Mendoza-Zelis, A. F. Pasquevich, F. H. Sanchez, and A. Lopez-Garcia, *Phys. Rev. B* **29**, 1109 (1984).
- ²⁷U. Bäverstam, R. Othaz, N. de Sousa, and B. Ringström, *Nucl. Phys. A* **186**, 500 (1972).
- ²⁸A. Abragam and R. V. Pound, *Phys. Rev.* **92**, 943 (1953).